

1994\_15

## ASSESSMENT OF TEMPERATURE-DRIVEN PRESSURE DIFFERENCES WITH REGARD TO RADON ENTRY AND INDOOR RADON CONCENTRATION

Kaiss K. Al-Ahmady and David E. Hintenlang  
University of Florida, Department of Nuclear Engineering Sciences  
Gainesville, FL

### ABSTRACT

A heavily instrumented and unoccupied research house is used to continuously monitor the temperature in each room, the supply and return ducts, HVAC thermostat location, attic and outdoors. Simultaneous measurements of the differential pressures have been performed across the house walls, indoor/attic zones, the house slab and the indoor zones. Indoor radon concentrations and meteorological conditions have also been monitored. Temperature measurements were conducted using thermocouple wires. All data were collected by computer-controlled data acquisition input boards. An analytical model was developed based on a linear approximation to the weakly exponentially dependent pressures between two temperature zones under hydrostatic equilibrium. The model is utilized to predict the temperature-induced pressure difference between two separated temperature zones. This model is then coupled with a semi-empirical formulation that utilizes pressure differences to predict radon entry into the structure and the air exchange rate across the house shell. The partial contributions of various temperature-induced pressure differences are assessed on the model driving parameters. The contribution to the indoor radon concentrations are then obtained by incorporating the predicted changes in pressure differentials into the mass balance equation governing the time rate changes of the radon concentrations. It has been demonstrated that temperature differences associated with extreme weather conditions can generate pressure differences of several pascals that profoundly contribute to radon driving forces and indoor radon concentrations. The partial contributions of temperature-driven radon entry rates and ventilation rates for a range of HVAC operation were also estimated.

### INTRODUCTION

The transport of radioactive radon gas from the sub-slab area into structures such as residential housing can be described by convective and molecular diffusion processes. The soil gas has emerged as the main source of indoor radon (Nero and Nazaroff 1984, Nazaroff et. al 1988a, Crameri et. al 1989). Radon ( $^{222}\text{Rn}$ ) entry into residential structures occurs principally through pressure driven airflow processes. These processes are induced by pressure differential generating mechanisms that depend on interactions among environmental and indoor operational factors. Typical environmental interactions result in sources of house depressurization, such as temperature, wind and stack effects. House depressurization contributes to an increase in indoor radon concentrations as  $^{222}\text{Rn}$ -rich soil gas entry rates are increased compared to the increase in the air infiltration rates (Nazaroff et. al 1987, Nero 1988). In many cases the concentrations of indoor radon exhibit a diurnal cycle driven by temperature dependent pressure differences (Gesell 1983, Kunz 1987).

Furrer et al. (1991) studied the dynamics of Rn transport from the cellar to the living area in an unheated house and found that strong, long-term correlations between temperature differences and pressure differences exist between the indoors and outdoors. Experimental verification, however, for this diurnal dependence is in most cases profoundly affected by uncontrolled pressure changes across the structure shell due to natural and mechanical ventilation caused by occupants' activities and/or the heating, ventilating and air conditioning (HVAC) system operation. Other researchers have given an increased importance to the transient effects of barometric pressure changes associated with changing meteorological conditions as contributors to radon driving forces (Owczarski et.

al 1990, Al-Ahmady 1992, Hintenlang and Al-Ahmady 1992, Tsang and Narsimhan 1992).

Al-Ahmady and Hintenlang (1993) had developed a mechanistic model to characterize the temperature-driven pressure differentials. The model is based on a linear approximation to the weakly exponentially dependent pressures between two temperature zones under hydrostatic equilibrium. In this work, the previous model is utilized to assess temperature induced pressure differences contribution into the radon driving forces including radon entry and removal. A mathematical framework is developed to integrate the temperature-induced pressure differences model (Al-Ahmady and Hintenlang 1993) into a semi-empirical model for radon entry and indoor radon concentration. The latter model was developed by Hintenlang and Al-Ahmady (1994) to predict the radon entry and indoor radon concentration by the providing of pressure differences across the house shell and the slab. Parametric analysis is provided to estimate the temperature effects on the radon entry driving forces under unoccupied, unheated conditions and under heated conditions as provided by the HVAC system.

The data presented were collected on the University of Florida Radon Research House (UFRRH) as part of the Florida Radon Research Program (FRRP). The research house was carefully chosen and heavily instrumented by a variety of devices. Thus, a number of key parameters could be measured or monitored simultaneously. The research effort by the University of Florida is dedicated to the development of building codes governing radon resistance for Florida houses and is designed to provide detailed characterization of the effects of HVAC on radon entry, as well as modeling of the radon entry and transport.

## METHODOLOGY

Continuous measurements have been taken, in order to track the time and spatial dependent responses of the temperature, pressure, radon concentrations, weather parameters, and HVAC operation parameters at the UFRRH. The house is an unoccupied one-story residential structure and has a floor area of 163 m<sup>2</sup>, utilizing a concrete slab-on-grade type of construction with a 10.1m x 16.2m footprint. The temperature and pressure data are collected using analog and thermocouple input boards integrated to a Keithley Metrabyte micro-channel driver card. A Setra 270 barometric pressure transducer (600-1100 mbar range) is installed at the site and is integrated to the Metrabyte data acquisition and control system. The Metrabyte system is interfaced with and fully controlled by an IBM PS/2 computer system.

The pressure differential measurements across the house walls, slab, and indoor locations are performed utilizing very low range Setra C264 differential pressure transmitters of  $\pm 25$  Pa full scale with a minimum sensitivity of less than  $\pm 0.25$  Pa. An array of sixteen pressure transmitters is distributed across the slab in a uniform 4.88m x 2.74m grid pattern. These transmitters monitor the differential pressure above and below the concrete slab through standard 4.7 mm I.D. tubes that provide access to the sub-slab area at each grid point.

Every exterior pressure port (that for barometric pressure and those penetrating the walls) is covered by a perforated, hollow sphere to dampen rapid pressure variations caused by wind gusts. The measurements between the outdoor and the sub-slab are performed using T-section link tubing at one of the sub-slab points. The transmitters are connected to the Metrabyte system using an Omega switchboard to provide flexibility during calibrations and to run the measurements at specific slab points as needed. All pressure transmitters are "zero checked" at the beginning of each experimental period and calibrated monthly.

Temperature is monitored in each room, at the supply and return ducts, room register, HVAC thermostat location, attic, sub-slab area, and outdoors, using T-type, copper vs. copper-nickel, thermocouple wires. The Metrabyte thermocouple board cold junction temperature is calibrated at the beginning of each measurement period. The weather parameters such as wind speed, wind direction and rainfall data are collected utilizing a datalogger integrated to a meteorological station located at the site and compiled remotely for processing.

The measurements of indoor radon concentrations are performed using AT-Ease, E-PERM, and Pylon radon measuring systems. The time dependent radon measurements are performed using Pylon AB-5 portable radon monitors utilizing the passive radon detector cell (PRD-1). The Pylon counts are accumulated over a time interval, stored in the monitor memory at the end of each interval, and downloaded to an IBM PC at the conclusion of the experimental period.

An experimental period of 96 hours and a measurement interval of 60 seconds, averaged every 600 seconds, have been used to perform the measurements. These periods provide a suitable time in which to monitor both the transient response in the house system and the response upon house system stabilization. The same experimental protocol is followed for each experimental period.

## RESULTS AND DISCUSSION

Differential pressure measurements between the indoors and outdoors and between the indoors and the sub-slab area over an interval of 48 hours at the UFRRH are illustrated in Figure 1. The two differential pressure responses do not appear to be coupled to each other. The differential pressures across the floor slab have larger magnitudes and are dependent on the geometrical location under the slab. Higher pressures are usually found near the center of the slab, while lower ones are located near the slab edges.

The indoor/outdoor pressure differential response demonstrates a diurnal cycle with a peak amplitude of about 0.4 Pa. This is attributed to the variation in temperature difference between the indoor and outdoor environments that occurs throughout the day. These responses are small in magnitude because temperature differences between the indoors and outdoors remain small during the time of year, in which these experiments were performed, and also because the house is well sheltered from the wind. The minimal contribution of wind effects is verified by the weather station mounted on the structure and by the indoor/outdoor differential pressure monitors mounted on two opposite sides of the house. The anemometer indicates wind speeds of less than 0.18 m/s greater than 90% of the time, and the indoor/outdoor pressure responses measured across the different walls were observed to be nearly identical (in phase) throughout the experimental periods. This demonstrates that the influence of wind induced pressure imbalances during these experiments is insignificant.

Temperature differences between the indoors and the outdoors can cause air volume movements corresponding to the temperature gradient and, consequently, pressure differences. Further, temperature differences across walls separating air masses can cause pressure differences. The pressure differences in the last case vary with the wall height. This phenomenon is known as the stack effect. Nazaroff et al. (1987) performed experiments by inducing depressurization in two residential structures with basements to simulate the depressurization that can be generated by wind and temperature differences. They concluded that nearby soil pressure field and air movements are influenced by the induced depressurization in the structures. They also reported on the possibility that these effects may account for the higher than average indoor radon concentration observed in these two houses with basements.

The stack effect, resulting when air masses of different temperatures are separated by a wall, can provide airflow pressure driven force to the convective component of radon transport into structures. This effect should exist principally at the wall-slab interfaces, causing a buoyant effect that draws air from the soil into the lower part of the structure and pushes it out through the upper part. It is believed that this mechanism increases the outdoor-indoor pressure differences and increases the indoor radon concentrations (Nero 1988, Nazaroff et al. 1988b).

Pressure differentials between the indoor and sub-slab air volume pressures,  $\Delta P_{\text{sub}}$ , vary with approximately a semi-diurnal periodicity and have a significantly greater magnitude than the indoor/outdoor pressure differential,  $\Delta P_{\text{io}}$ , (Al-Ahmady 1992, Hintenlang and Al-Ahmady 1992). The soil system below the structure slab heavily damps the response of the sub-slab air volume pressure to changes in barometric pressure, particularly for houses built over low permeability soils. The indoor pressure responds much faster, creating pressure differentials across

the floor slab. These pressure differentials provide a driving force that naturally pumps radon-rich soil gas from the sub-structure area into the interior during the part of the cycle when the house indoor pressure is lower than the sub-structure air volume pressure, causing elevated indoor radon concentrations.

Recent studies have shown particular importance of this phenomenon when it is associated with the HVAC system design and operation (Hintenlang and Al-Ahmady 1993). It has been demonstrated that increasing the house ventilation rate by increasing the effective leakage area of the house shell does not reduce indoor radon concentrations as effectively as increasing house ventilation rate by controlled duct ventilation associated with the HVAC system (Hintenlang and Al-Ahmady 1994).

Temperature measurements in several locations at the research structure taken simultaneously with the barometric pressure and the differential pressure measurements showed indoor temperatures response with only small variation and forms a flat spacial distribution at a given height in the indoor environment. Therefore, the research structure living space may be considered a single thermal zone with the indoor temperature,  $T_i$ , calculated as the average of the temperature measurements from all of the indoor points. With the house un- air conditioned and unoccupied, there is a time shift in the response of the indoor temperature to changes of the outdoor temperature,  $T_o$ . Such a time shift is also sometimes observed between the indoor temperature and the attic or sub-slab temperature. This shifting depends on several factors, such as the structure's thermal properties, the interactions between the structure's thermal zones, the magnitude of the ambient temperature changes, and the shell configuration. These time responses may be found to have particular importance in shaping the radon driving force when the time response between the sub-slab air volume pressure and the indoor pressure are considered. The temporal variations of indoor/outdoor ( $T_i-T_o$ ) and indoor/sub-slab ( $T_i-T_u$ ) temperature differences are shown in Figure 2. For an inhibited, un- air conditioned, home the maximum indoor-outdoor temperature difference of about 9 °C was observed at the time of this experiment, when the house undergoes a positive temperature difference (the indoor temperature exceeds the outdoor temperature) for approximately 75% of the day. During mild weather (Data collected during march in Gainesville, FL) the maximum and minimum temperatures occur at about 4 pm and 6 am, respectively. The maximum/minimum temperatures and the temperature differences depend on the time of the year and the particular location. Therefore, the temperature effects are also important in studying the seasonal effects on radon driving forces and consequently the indoor radon concentrations.

The force associated with a fluid pressure, such as air pressure, must counteract the gravitational force under hydrostatic equilibrium. For a specific volume, the net force at any point must be zero. Therefore,

$$dP/dh = -\rho g \quad (1)$$

where  $h$  is the height measured from a reference level (m),  $\rho$  is the air density ( $\text{kg/m}^3$ ), and  $g$  is the gravitational acceleration constant (9.8 m/s). Air can be consider to be an ideal gas for this application. Utilizing the universal gas law, the air density is,

$$\rho = P/RT \quad (2)$$

were  $R$  is the universal gas constant then,

$$dP/dh = -P(mg/kT) \quad (3)$$

were  $m$  is the mass of air (kg),  $k$  is Boltzmann constant ( $1.38 \times 10^{-23}$  J/K), and  $T$  is the absolute temperature (K). If boundary conditions established as  $P = P_o$  at  $h = 0$ , the solution to the first order differential equation above yields,

$$P = P_o \exp(-mgh/kT) \quad (4)$$

The change in  $P_o$  is negligible at heights encountered in a single-story residential structures. If the temperature

measurements are established at a constant height from the slab and the outside, the pressure value can be correlated to the temperature changes. At the research structure temperatures were measured at 1.4 m above the slab ( $h=1.4$  m). The magnitude of  $mgh/k$  is a constant of value  $B=0.0477$  K, when  $m$  is the average molecular mass of air (28.8 u) at an atmospheric composition of approximately 80%  $N_2$  and 20%  $O_2$ , at uniform temperature of 280 K. In most cases, the constant  $B$  is small, and the value  $\exp(-B/T)$  can be estimated as  $(1-B/T)$ . Applying this treatment to two pressure conditions  $P_1$  and  $P_2$ , which correspond to temperatures  $T_1$  and  $T_2$ , respectively, yields

$$P_1 - P_2 = \Delta P = P_o B [(T_1 - T_2)/T_1 T_2] \quad (5)$$

the pressure difference generated between two zones of different temperatures. Eqn. 5 can be used to predict temperature-induced pressure differences with regard to radon driving forces and indoor radon concentrations. The output predictions of the model is  $\Delta P$ , for the model input  $\Delta T$ , and it is suitable to many radon entry models that utilize  $\Delta P$  to predict radon entry rate. This output is also suitable to most of the structure ventilation models that utilized  $\Delta P$  to predict the structure natural infiltration and ventilation rates.

Integration of the above model into a radon entry and indoor radon concentration semi-empirical model (Hintenlang and Al-Ahmady 1994) was performed to observe the temperature effects on radon driving forces. This model was developed for the UFRRH and consequently the constant values used characterize the effective leakage area and the characteristic slab openings at the UFRRH. Convective components for radon entry into the structure are radon entry from the sub-slab area and from the ambient environment. The convective component of radon entry from the sub-slab soil area into the interior was obtained by simultaneously measuring the time-dependent pressure differentials across the slab and the indoor radon concentration. Experimental values were used when temperature measurements between the indoor and outdoors showed approximately equal and flat responses. The experimental fit to simultaneous  $\Delta P$  measurements and indoor radon concentrations provides,

$$R_u = 13.32 \Delta P_{sb} \quad (6)$$

where  $R_u$  is the sub-slab radon entry rate. The ambient radon entry into the structure was obtained from blower door testing to the UFRRH structure following the ASTM standards (ASTM 1987) as,

$$R_{amb} = 1.07(\Delta P_{vo})^{0.69} \quad (7)$$

$R_{amb}$  is the radon entry rate from the outdoors. Radon entry by diffusion is independent from the convective components although it is a part of the total radon entry rate.

The steady state solution to the time-dependent mass balance equation for indoor radon concentration can be written as (Hintenlang and Al-Ahmady 1994),

$$C = R/(Q + \lambda V) \quad (8)$$

where  $R$  is the total radon entry rate (Bq/s),  $Q$  is the structure ventilation rate ( $m^3/s$ ),  $\lambda$  is the radioactive decay constant of  $Rn-222$ ,  $V$  is the indoor volume ( $m^3$ ), and  $C$  is the steady state indoor radon concentration (Bq/ $m^3$ ). The structure ventilation rate was calculated by the blower door testing (ASTM 1987) and empirically fitted to,

$$Q = 0.056 (\Delta P_{vo})^{0.69} \quad (9)$$

Utilizing Eqns. 5, 6, & 7 the convective radon entry rate can be written as,

$$R_{conv} = P_o B \{ 1.07 (P_o B)^{-0.31} [(T_1 - T_o)/T_1 T_o]^{0.69} + 13.23 [(T_1 - T_u)/T_1 T_u] \} \quad (10)$$

where  $T_u$  is the sub-slab air volume temperature and  $R_{conv}$  is convective radon entry rate. In the special cases when

weather patterns permit the sub-slab air volume temperature equals to the outdoor temperature, then

$$R_{\text{conv}} = P_o B T [13.23 + 1.07 (P_o B)^{0.31} T^{0.31}] \quad (11)$$

were  $T$  is  $(T_i - T_o)/T_o$ . Utilizing Eqns. 8,9, &10 the contribution of temperature-induced pressure differentials to the steady state indoor radon concentrations can be assessed provided that temperature correction be made for the structure ventilation.

Figure 3 illustrates the indoor/outdoor pressure differences, which are induced by the indoor/outdoor temperature differences, given by Eqn. 5. The predicted values of the pressure differential between the indoors and outdoors are in good agreement with the ones measured at the site for the same time interval. Figure 4 shows the model predictions for pressure differences induced over a range of temperature differences. Induced pressure differences between the indoors and outdoors show a linear correlation to the corresponding temperature differences. It is important to note that the model shows that these pressure differences are sensitive not only to the temperature differences, but also to the average temperature between the indoors and outdoors. However, this dependence might be enhanced by the mathematical treatment in the model. The value of  $P_o$  was calculated at the UFRRH slab level with a standard air composition at uniform temperature of 280K and kept constant. This dependency needs further investigation to see if it can be offset by the change in  $P_o$  value when adjustment in  $P_o$  is made based on the average temperature between the indoor and outdoors.

The effect of the temperature on the sub-slab air volume pressure is expected to be smaller than its effect on indoor pressure, based on temperature measurements at the UFRRH between the indoors and the sub-slab which show maximum differences of about 2 °C. These effects may be larger for different types of soil, different types of buildings, and different overall weather patterns. A positive temperature difference contributes to the indoor pressure and reduces the differential pressure across the slab, thereby reducing the natural pumping radon driving force. Figure 5 illustrates the temperature-induced pressure differences contribution into radon entry rate from the sub-slab area into the interior. The contribution from the diffusion component can be calculated by superimposing a constant value on the  $R_{in}$ . These are illustrated in Figure 5. At the UFRRH the average diffusion entry is 10 Bq/s. Figure 6 illustrates the effect of temperature-induced pressure differences on the structure ventilation parameters. The scope of HVAC induced temperatures is also covered.

## CONCLUSIONS

Indoor, outdoor and sub-slab temperature measurements at the UFRRH have shown periodic time variations with a diurnal cycle. The diurnal temperature differences between the indoors and outdoors are strongly correlated to diurnal pressure differences induced between the indoors and outdoors. The induced pressure differences are linearly proportional to the magnitudes of the temperature differences and to the average temperature between the indoors and outdoors. Temperature-driven pressure difference predictions can be performed by the use of linear approximation to the weakly exponentially dependent pressures of two temperature zones under hydrostatic equilibrium. An analytical model can be constructed to output pressure differences in response to temperature difference inputs. Since the model output is pressure differences, integrations into radon entry and indoor radon concentration predictions models are systematic. Temperature-driven pressure differences model can be integrated into models inputs pressure differences to assess the temperature effects on radon entry rate from the sub-structure area and from the ambient into the interior. Assessment to the radon removal rate can be characterized by calculating the temperature effects on the natural and mechanical ventilation rates of the structure. Consequently, the combination of the radon removal and entry rate can be used to assess the indoor radon concentration. Temperature-differences encountered with the use of the heating, ventilating and air conditioning (HVAC) system may produced pressure differences of the same order of radon entry driving forces observed in slab-on-grade residential structure built under low permeability soil and fill materials. Such differences, therefore, could profoundly influence radon entry and indoor radon concentrations.

## REFERENCES

Al-Ahmady, K.K. "Measurements and Theoretical Modeling of A Naturally Occurring  $^{222}\text{Rn}$  Entry Cycle For Structures Built Over Low Permeability Soils", Master of Engineering Thesis, University of Florida, Gainesville, Florida; 1992.

Al-Ahmady, K.K. and Hintenlang D.E. "Measurements and Theoretical Modeling of Diurnal Temperature Effects on The Natural Periodic Atmospheric Pressure Variations Driven Radon Entry into Structures Built Over Low Permeability Soils", Accepted for Presentation, The 16th World Energy Engineering Congress, The Association of Energy Engineers; 1993.

American Society for Testing and Materials "Standard Test Method for Determining Air Leakage Rate By Fan Pressurization", Philadelphia, PA, ASTM, ASTM E779-87; 1987.

Cramer, R.; Brunner, H.H.; Buchli, R.; Wernli, C.; Burkart, W. "Indoor Rn Levels in Different Geological Areas in Switzerland", *Health Physics*, 57:29-38; 1989.

Furrer, D.; Cramer, R. and Burkart, W. "Dynamics of Rn Transport From The Cellar To The Living Area in an Unheated House", *Health Physics*, 60:393-398; 1991.

Gesell, T.G. "Background atmospheric  $^{222}\text{Rn}$  concentrations outdoor and indoors: A review", *Health Physics*, 45:289-302; 1983.

Hintenlang, D.E.; Al-Ahmady, K.K. "Pressure Differentials for Radon Entry Coupled to Periodic Atmospheric Pressure Variations", *Indoor Air*, 2:208-215; 1992.

Hintenlang, D.E. and Al-Ahmady, K.K., "Building Dynamics and HVAC System Effects on Radon Transport in Florida Houses", *The 1992 International Symposium on Radon and Radon Reduction Technology*, Vol. 1:VI:93-106, EPA-600/R-93-083a, Springfield, VA. NTIS PB93-196194, 1993.

Hintenlang, D.E.; Al-Ahmady, K.K. "Influence of Ventilation Strategies on Indoor Radon Concentrations Based on a Semi-Empirical Model for Florida-Style Houses", *Health Physics*, 66:427-432; 1994.

Kunz, C. "Indoor Radon: The diurnal Cycle", *Indoor Air*, 87, Vol 2, Proceeding of The 4th International Conference on Indoor Air Quality and Climate, Berlin (west); 17-21 August 1987, Berlin: Institute for Water, Soil and Air Hygiene, 415-418; 1987.

Nazaroff, W.W.; Lewis, S.R.; Doyle, S.M.; Moed, B.A.; Nero, A.V. "Experiments on Pollutant Transport from Soil into Residential Basements by Pressure-Driven Airflow", *Environmental Science and Technology*, 21:459-466; 1987.

Nazaroff, W.W.; Moed, B.A.; Sextro, R.G. "Soil as a Source of Indoor Radon: Generation, Mitigation and Entry, In: *Radon and its Decay Products in Indoor Air*", Nazaroff, W.W.; Nero, A.V., eds., John Wiley & Sons, New York, 57-112; 1988a.

Nazaroff, W.W.; Feustal, A.; Nero, A.; Revzan, K.L.; Grimsrud, D.T.; Essling, M.A.; Toohey, R.E. "Radon Transport into a Detached One-Story House with a Basement", *Atmospheric Environment*, 19: 31-46; 1988b.

Nero, A.V.; Nazaroff, W.W. "Characterizing The Source of Radon Indoors", *Radiation Protection Dosimetry*, 4: 23; 1984.

Nero, A. V. "Radon and Its Decay Product in Indoor Air: An Overview, In: Radon and its Decay Products in Indoor Air", Nazaroff; W.W., Nero, A.V., eds., John Wiley & Sons, New York, 1-52; 1988.

Owczarski, P.C.; Holford, D.J.; Freeman, H.D.; Gee, G.W. "Effects of Changing Water Content and Atmospheric Pressure on Radon Flux From Surfaces of Five Soil Types", *Geophysical Research Letters*, 17, 6: 817-820; 1990.

Tsang, Y.W.; Narsimhan, T.N. "Effects of Periodic Atmospheric Pressure Variation on Radon Entry into Buildings", *Journal of Geophysical Research*, 97(B6):9161-9170; 1992.

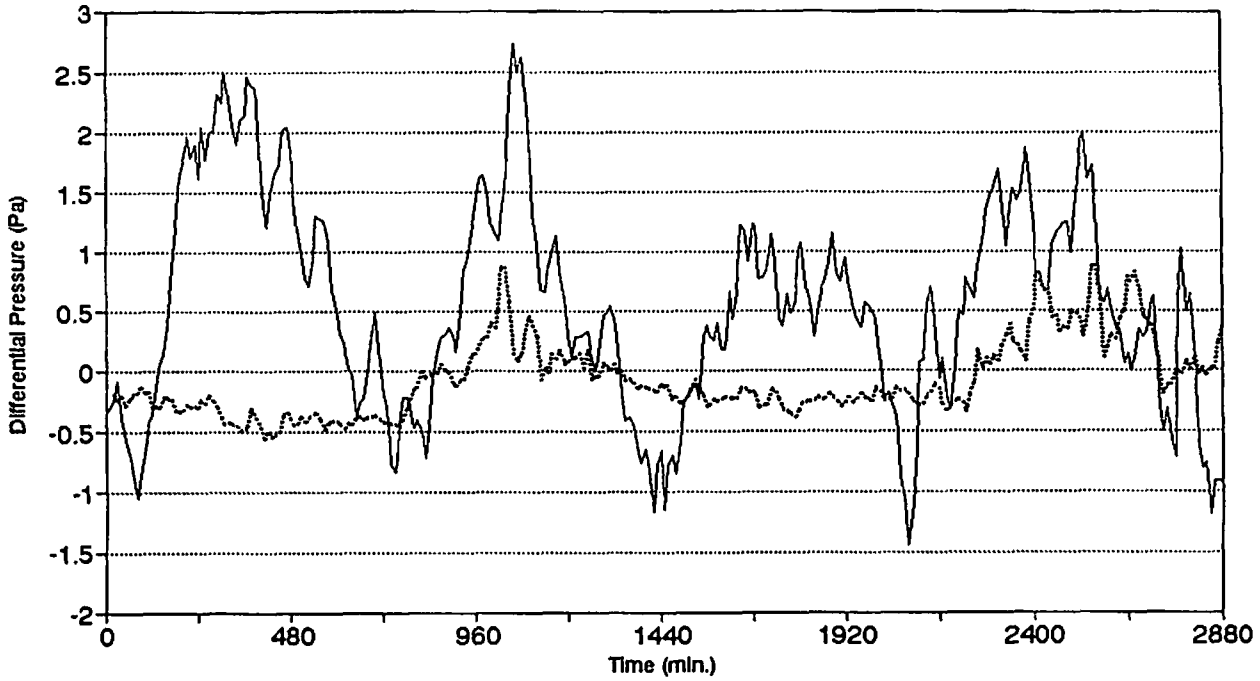


Fig. 1: Time Variation of The Average Differential Pressures Between The Indoors and Sub-Slab (Solid Line) and The Indoors and Outdoors Under Unoccupied Neutral Pressure Conditions.

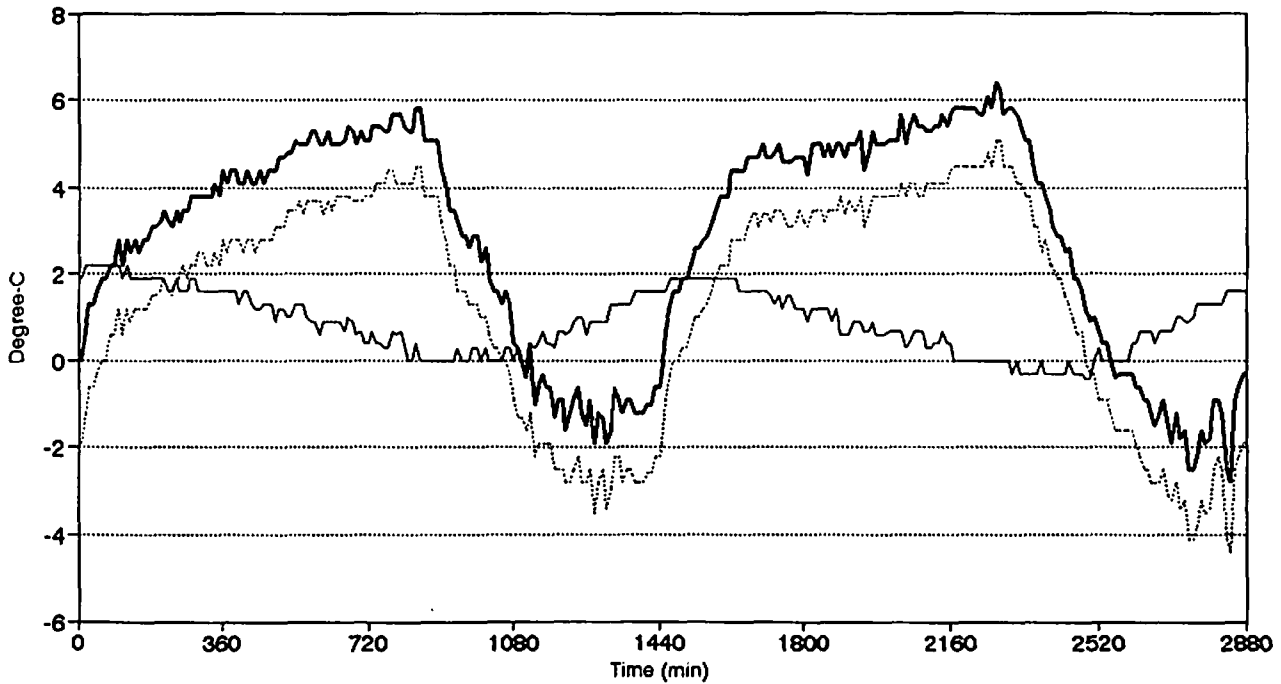


Fig. 2: The Temporal Variations of Temperature Differences At The UFRRH: Indoor/Outdoor (Heavy Solid), Indoor/Sub-Slab (Solid) and Attic/Outdoor.

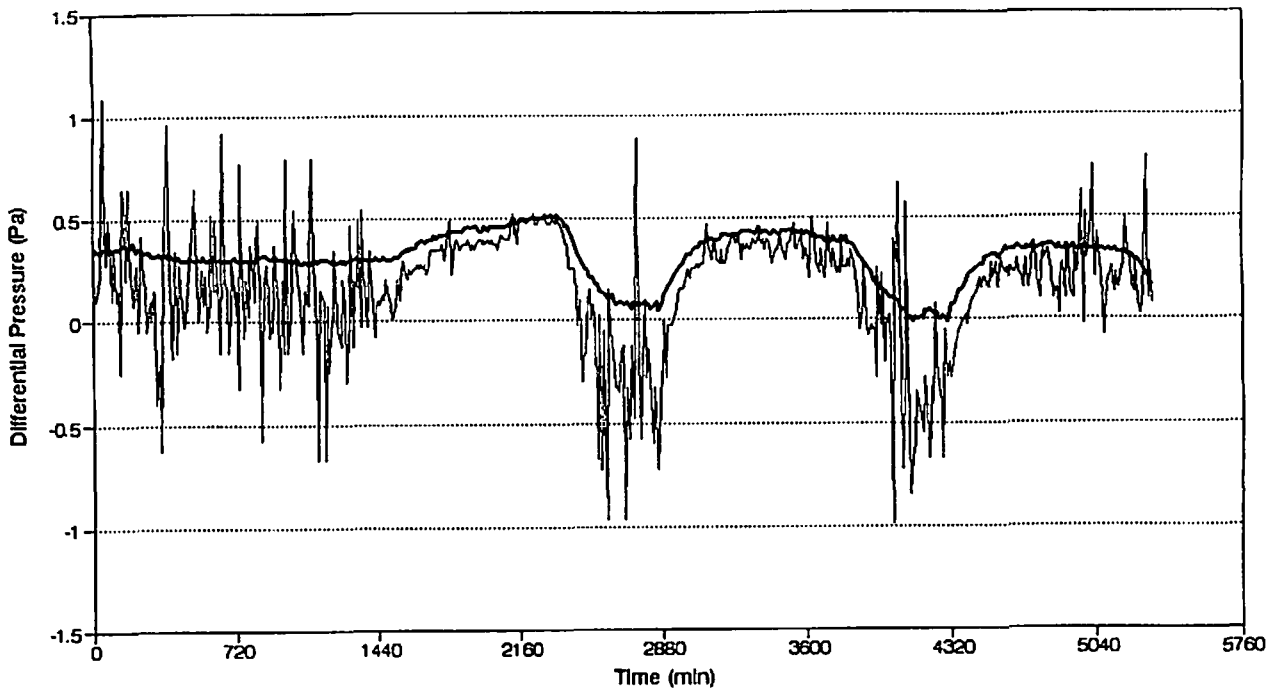


Fig. 3: Indoor/Outdoor Pressure Differences (Modeled, Solid Line; Measured Soft Line) Induced By The Time Variations of Indoor/Outdoor Temperature Differences.

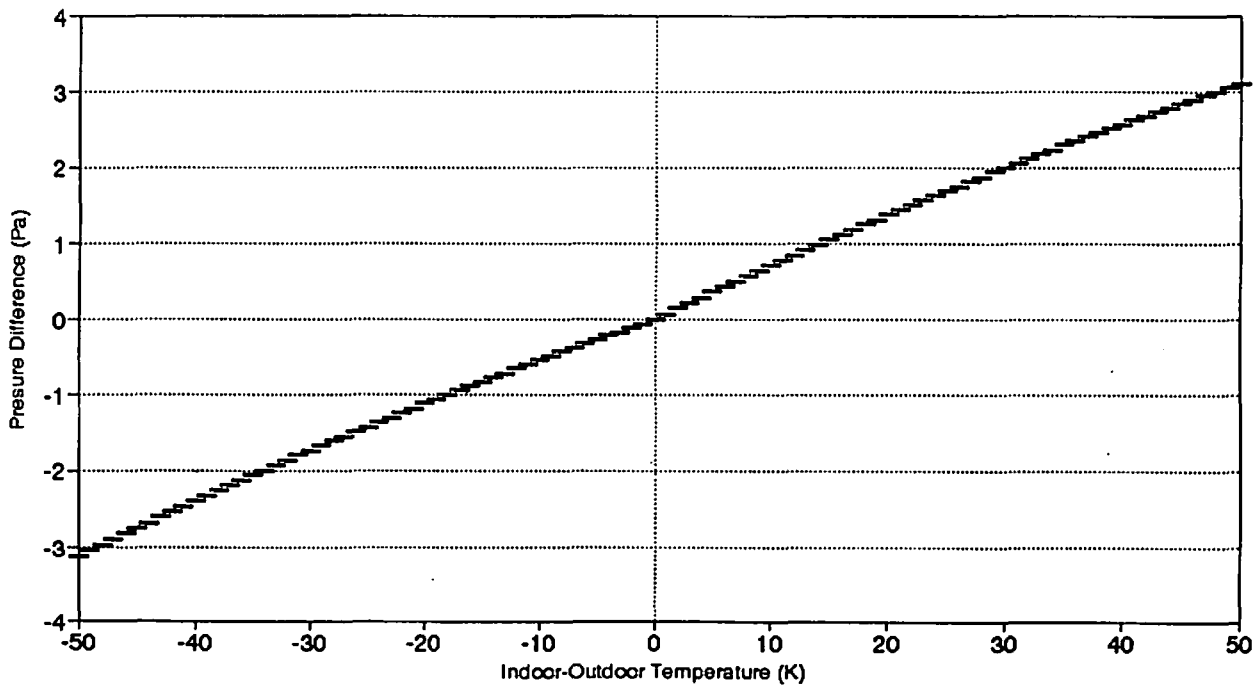


Fig. 4: The Model Predictions of The Temperature Induced Pressure Differential Between The Indoors and Outdoors as a Function of The Indoor/Outdoor Temperature Differences.

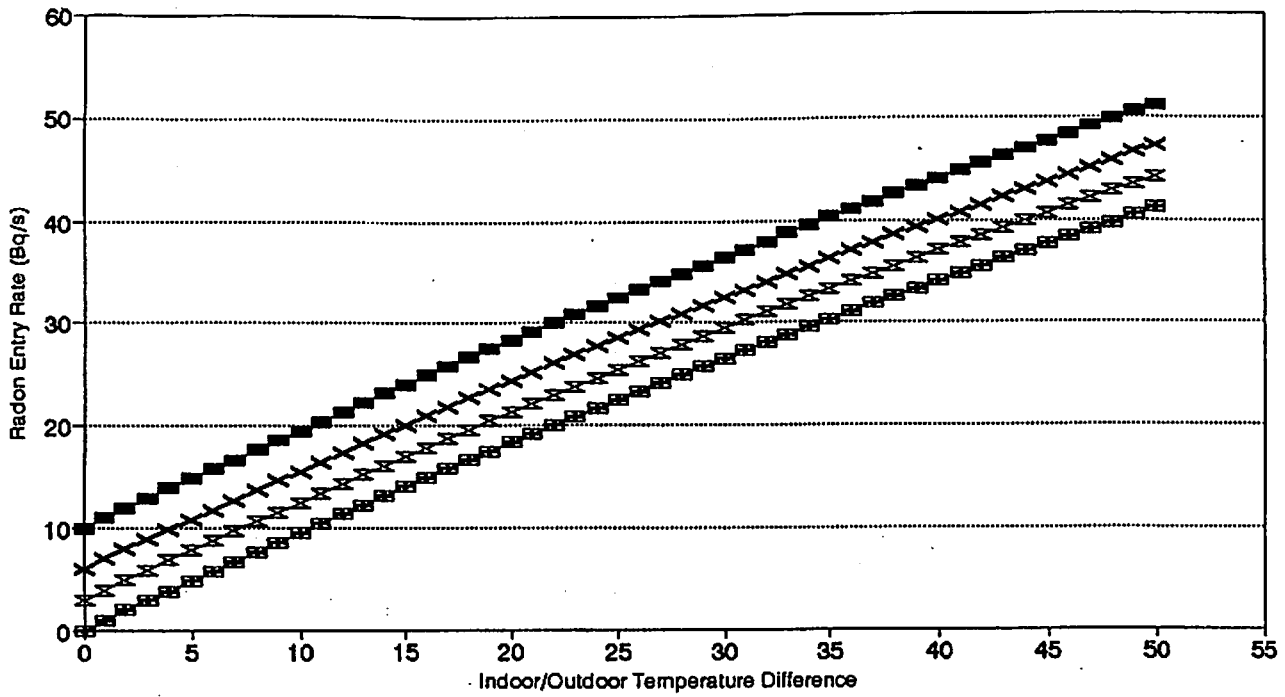


Fig. 5: Predictions of The Radon Entry Rate From The Sub-Slab Area into The Interior Generated By Temperature-Induced Pressure Differences. (Bottom to Top: No Diffusion Entry, Constant Diffusion Entries of 3, 6, & 10 Bq/s, respectively).

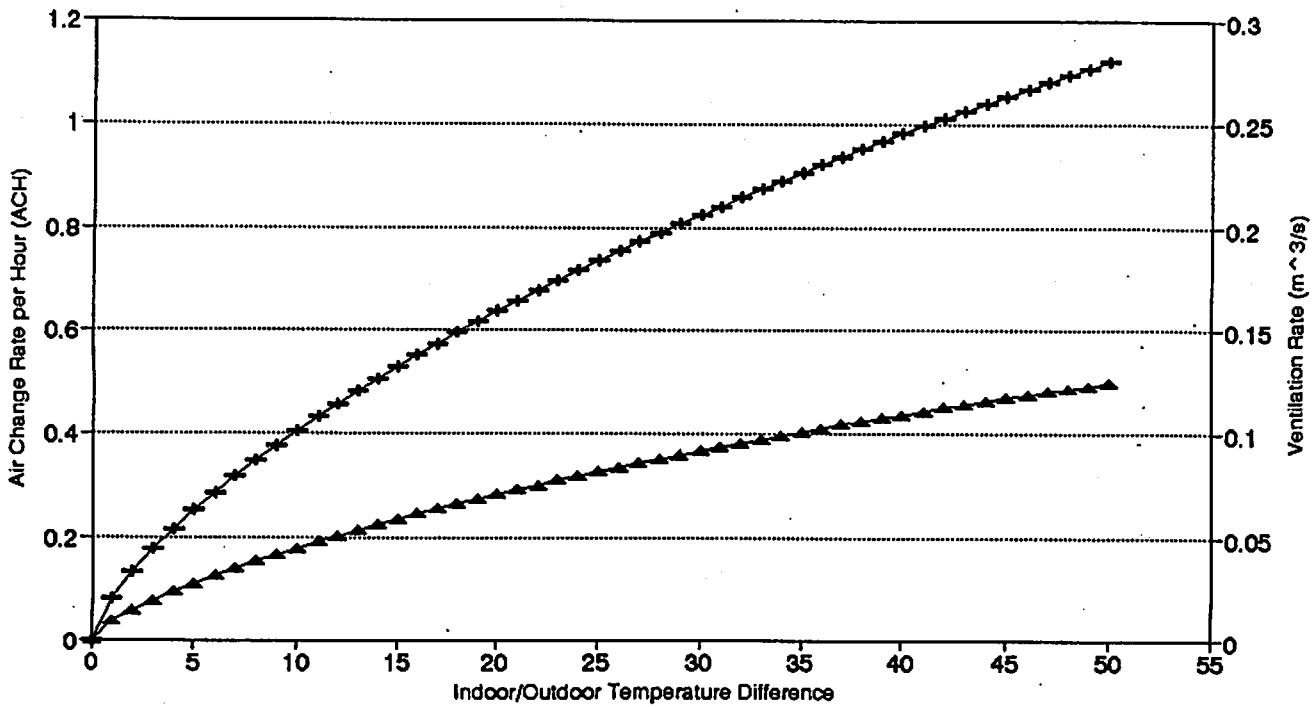


Fig. 6: The Effect of Temperature-Induced Pressure Differences on The Structure Ventilation Rates (ACH- Plus Sign).